

1  
2  
3  
4  
5  
6  
7  
8  
9  
10  
11  
12  
13  
14  
15  
16  
17  
18  
19  
20  
21  
22  
23  
24  
25  
26  
27

## **Exploitation by cheaters facilitates the preservation of essential public goods in microbial communities**

Clara Moreno-Fenoll<sup>1</sup>, Matteo Cavaliere<sup>1,2</sup>, Esteban Martínez-García<sup>3</sup>, Juan F. Poyatos<sup>1\*</sup>

<sup>1</sup>Logic of Genomics Systems Lab (CNB-CSIC), Madrid Spain

<sup>2</sup>University of Edinburgh, Edinburgh, UK

<sup>3</sup>Molecular Environmental Microbiology Lab (CNB-CSIC), Madrid, Spain

\*Correspondence to: [jpoyatos@cnb.csic.es](mailto:jpoyatos@cnb.csic.es)

## 28 **Summary**

29

30 How are public goods<sup>1-4</sup> maintained in bacterial cooperative populations? The presence of  
31 these compounds is usually threatened by the rise of cheaters that do not contribute but  
32 just exploit the common resource<sup>5,6</sup>. Minimizing cheater invasions appears then as a  
33 necessary maintenance mechanism<sup>7,8</sup>. However, that invasions can instead add to the  
34 persistence of cooperation is a prospect that has yet remained largely unexplored<sup>6</sup>. Here,  
35 we show that the detrimental consequences of cheaters can actually preserve public goods,  
36 at the cost of recurrent collapses and revivals of the population. The result is made  
37 possible by the interplay between spatial constraints and the essentiality of the shared  
38 resource. We validate this counter-intuitive effect by carefully combining theory and  
39 experiment, with the engineering of an explicit synthetic community in which the public  
40 compound allows survival to a bactericidal stress. Notably, the characterization of the  
41 experimental system identifies additional factors that can matter, like the impact of the lag  
42 phase on the tolerance to stress, or the appearance of spontaneous mutants. Our work  
43 emphasizes the unanticipated consequences of the eco-evolutionary feedbacks that emerge  
44 in microbial communities relying on essential public goods to function, feedbacks that  
45 reveal fundamental for the adaptive change of ecosystems at all scales.

46

47

48

49

50

51

52

53

54

55

## 56 **Main text**

57

58           The threat of cheaters represents at a microbial scale a well-known public good  
59 (PG) dilemma, known as the "tragedy of the commons"<sup>9</sup>, and can fundamentally interfere  
60 with the sustainability of microbial communities. The necessity of recognizing the  
61 consequences of social dilemmas in microorganisms thus becomes essential, given their  
62 impact in many aspects of life on Earth, and also its particular relevance to humans in  
63 matters of health (microbiome)<sup>10</sup>, and industry (bioremediation, biofuels, etc)<sup>11</sup>. We  
64 considered specifically a scenario in which a community is organized as a dynamical  
65 metapopulation (i.e., the community is transiently separated into groups)<sup>12</sup>, and the action  
66 of a PG is essential for its survival. Spatial structure is a well-known universal mechanism  
67 to promote cooperation<sup>13</sup>, which frequently emerges in bacterial populations, for instance,  
68 due to the restricted range of microbial interactions<sup>14,15</sup>. However, it is much less  
69 understood how the presence of structure affects the maintenance of cooperation when  
70 combined with explicit population dynamics (earlier work usually assumed constant  
71 population and only examined evolutionary dynamics)<sup>16</sup>. The change in population size  
72 associated to the essentiality of the PG can indeed bring about complex eco-evolutionary  
73 feedbacks<sup>17-20</sup>, in which both population density and frequency of "cooperators" influence  
74 each other. The connection between these feedbacks and spatial structure remains thus an  
75 open problem that has started to be addressed only recently<sup>21-22</sup>. We show in this work  
76 how such connection can direct to the unforeseen consequence that cheater invasions  
77 eventually support cooperation.

78

79           To analyze this scenario, we first introduced a stylized *in silico* model considering  
80 an initial finite population of agents -representing bacteria- with a given frequency of  
81 cooperators (producers of a PG, with a fitness cost) and cheaters (nonproducers, that  
82 could have emerged originally from the cooperators by mutation)(Methods). The  
83 population is temporarily organized in groups, where interactions take place (fig. S1).  
84 These interactions are modelled by means of a PG game with individual reproduction  
85 being set by the game payoff<sup>17,18</sup>. Figure 1A displays a representative trajectory of the  
86 model: an increase of the cheating strain, due to its fitness advantage, causes a decrease in

87 population density (less PG available). The demographic fall originates in the end  
88 variation in the composition of the groups, facilitating population assortment and the  
89 appearance of pure cooperator/cheater groups. Since the groups uniquely constituted by  
90 cooperators grow larger, they can ultimately reactivate the global population promoting  
91 again new cheater invasions. The whole process manifests in this way as a continuous  
92 cycle of decay and recovery of the community (Figs. 1A-B) (Methods). Demographic  
93 collapses consequently turn into an endogenous ecological mechanism that causes the  
94 required intergroup diversity, supporting the overall increase of cooperators by means of a  
95 statistical phenomenon known as Simpson's paradox<sup>12,22</sup>. To underline that an endogenous  
96 ecological process naturally induces the variance that finally rescues cooperation, we  
97 introduced the notion of "ecological Simpson's paradox".

98

99 We then tested these ideas experimentally, by engineering a synthetic PG  
100 interaction that is essential for the survival of a microbial population to a bactericidal  
101 antibiotic (Fig. 1C). Specifically, we constructed an experimental system in which a  
102 synthetic *Escherichia coli* strain (the cooperator/producer) constitutively secretes an  
103 autoinducer molecule acting as PG. This molecule is part of a *quorum-sensing* (QS)  
104 system foreign to *E. coli*, which includes a cognate transcriptional regulator. We  
105 connected this machinery to the expression of a gene that enables the synthetic strain to  
106 tolerate the bactericidal antibiotic gentamicin (gm) (fig. S2, the system is a variation of an  
107 earlier one<sup>22</sup>)(Methods). A second strain (the cheater/nonproducer) that only utilizes the  
108 PG can also be part of the community (we labelled the cooperative and cheater strains  
109 with a green and red fluorescent protein, respectively, to make possible population  
110 measures) (Methods). Two crucial aspects distinguish in this way the designed setup.  
111 First, the presence of PG becomes an essential requirement to tolerate stress (Fig. 1D)  
112 (fig. S3). Second, the system exhibits an intrinsic vulnerability, as cheaters could  
113 overtake the entire community since they evade the cost of producing the PG (Fig. 1E)  
114 (fig. S4). While in this case the presence of cheaters is part of the synthetic design, their  
115 emergence as result of mutations is well documented in natural settings<sup>5,6</sup>.

116

117           The validation of the presented ecological Simpson's paradox is done using a  
118 minimal experimental protocol integrating the most important features of the model: the  
119 demographic collapse induced by cheaters, and the subsequent recovery of cooperation  
120 supported by the spatial constraints, i.e., the metapopulation. Specifically, the protocol  
121 includes two growing periods of PG accumulation and later exposure to stress (gm).  
122 Densities of cooperators and cheaters are quantified by plating (Methods). Both the *in*  
123 *silico* model and the main attributes of the experimental system predict that a community  
124 with different frequency of cooperative and noncooperative strains would accumulate a  
125 distinct amount of PG, and thus present different tolerance to stress. To confirm this, we  
126 engineered an initial population with density  $\sim 10^4$  cells/ml and different composition (fig.  
127 S5)(Methods). Figure 2A confirms the differential tolerance to stress (inset illustrates the  
128 resultant range of accumulation of QS molecules), whereas Fig. 2B additionally shows the  
129 effect on tolerance of rising the strength of stress for a fixed composition (20%  
130 cooperators). Note that the fraction of producers in these final populations does not vary  
131 substantially (fig S6).

132

133           Next, by distributing the initial full population into a metapopulation structure -  
134 before the rounds of QS accumulation and stress- we showed experimentally the basic  
135 features of the ecological Simpson's paradox. In particular, we selected as initial  
136 conditions the ones obtained after a large mixed population experienced a first round of  
137 comparatively strong stress (Fig. 2B, outcomes of an earlier round with a initial density of  
138  $\sim 10^4$  cells/ml constituted by 20% producers). As in the model, the reduced accumulation  
139 of PG in the mixed population causes a demographic collapse, which depends on how  
140 essential the PG becomes (the strength of stress). We considered explicitly the resulting  
141 populations after experiencing a medium (9.5 $\mu$ g/ml) and strong (13 $\mu$ g/ml) gm stress.  
142 These corresponded on average to  $\sim 24$  cfu/ml, and  $\sim 8$  cfu/ml, respectively (in what  
143 follows, we labelled them as "pop 1" and "pop 2"; the frequency of cooperators remains  
144  $\sim 20\%$ ). When we subsequently implemented a second round of the protocol with these  
145 initial population conditions, and the corresponding (medium and strong) gm dosages, we  
146 obtained two drastically different initial metapopulation distributions (Fig. 2C) (fig. S7).  
147 Notably, a low-density population ("pop 2") generates groups with very few cells and

148 assortment of cooperators, which is the group class that best tolerate stress (the  
149 characteristic behavior of this class is shown in Fig. 2D). Moreover, mixed groups and  
150 those composed by only cheaters do not grow, on average, with strong gm dosage (Fig.  
151 2D) (fig. S8). In this way, when all the groups of the metapopulation are pooled together,  
152 cooperators typically increase in frequency and population density recovers, in what is a  
153 manifestation of the ecological Simpson's paradox previously described (fig. S8)  
154 (Methods). Hence, the demographic decay of the population caused by the invasion of  
155 cheaters reveals crucial to attain the necessary heterogeneity among the various groups,  
156 and allows the recovery of cooperation. For a large population, groups exhibit a similar  
157 composition, on average, and as a result the behavior in the occurrence of the  
158 metapopulation is the same as in the absence of any structure, i.e., every well is in effect a  
159 replica of the same condition.

160

161 Two additional constraints could modify the dynamics above, which associate to  
162 general aspects of resistance and tolerance to antibiotic stress<sup>23</sup>. The first one identifies a  
163 possible trade-off between the build up of PG and the lag time of bacteria before exposure  
164 to the antibiotic. As Fig. 2A illustrated, the more PG a population accumulates (i.e., the  
165 longer it grows), the more it tolerates stress. However, when extensive growth implies a  
166 deterioration of the environmental conditions, PG could lose its functional activity<sup>24</sup> (Fig.  
167 3A)(fig. S9). Growing too much could be problematic. Moreover, when a bacterial  
168 population stays some time in saturating conditions, it presents a longer lag phase that  
169 indirectly protects bacteria from antibiotics<sup>23</sup>, independently on whether PG is available or  
170 not (Fig. 3A). Within the previous context of the recovery due to the ecological  
171 Simpson's paradox (Fig. 2C-D), low initial densities assure a regime further from  
172 saturation at the end of the accumulation period. This implies less decay of the PG and  
173 shorter lag, i.e., revival is under these conditions mostly linked to the action of the PG.  
174 The second constraint relates to the spontaneous emergence of mutants, which can resist  
175 the antibiotic and thus enable recovery of cheater populations in the absence of PG. This  
176 type of rescue is more difficult as the antibiotic dosage is increased, e.g.,<sup>25</sup> (fig. S10), and  
177 also underlines a constraint on the accumulation time of PG (the longer this period, the  
178 bigger the population and the chance for a mutant to arise) (Fig. 3B-C). Of note, both of  
179 these restrictions are less significant when the collapse of the population is very strong

180 ("pop 2" situation), that is when the best conditions exist for the ecological Simpson's  
181 paradox.

182

183 This study emphasizes that the combination of spatial constraints and specific  
184 attributes of the PG (e.g., essentiality) can be crucial for the outcome of the eco-  
185 evolutionary dynamics in cooperative bacterial communities. This is important in  
186 circumstances where the PG aids tolerance to stress, when nonintuitive effects may  
187 appear: an increase in cheaters frequency, or AB dosage, can actually precede the  
188 recovery of cooperation in the population. The particular experimental setup also provides  
189 synthetic strains with essential public goods; an original tool to test the demographic risks  
190 of cheaters invasions and implement experimentally a microbial tragedy of commons<sup>9</sup>,  
191 where cooperation is tied to population survival. Our results show overall that in this  
192 framework, spatial constraints, growth phase and the emergence of noninteracting mutant  
193 clones are aspects that should be considered to fully appreciate the resilience of social  
194 interactions in bacterial populations. In addition, synthetic communities emerge as  
195 tractable experimental models in which to begin to understand the tight ecological and  
196 evolutionary feedbacks increasingly observed in ecosystems worldwide<sup>26</sup>.

197

## 198 **Supplementary Information**

199 Figures S1-S10

200 Table S1

201

## 202 **Acknowledgements**

203 We would like to thank John Chuang for strains, and A. Couce, R. Díaz-Uriarte, D. Bajic,  
204 A. Sánchez, A. Pascual, O. X. Cordero, and V. de Lorenzo for helpful discussions. This  
205 work was partially supported by grants from La Caixa Foundation PhD fellowships, the  
206 Spanish Ministry of Economy and Competitiveness, and the British Engineering and  
207 Physical Sciences Research Council.

## 208 **Figure Legends**

209 **Fig. 1.** Exploitation by cheaters contributes to the maintenance of cooperation. (A)  
210 Typical population dynamics obtained with an *in silico* model of a microbial community,  
211 which is organized as a transient metapopulation (fig. S1) (Methods). Growth depends on  
212 an essential public good (PG) produced by the "cooperator" individuals. When "cheaters"  
213 invade, the decline in the amount of PG drives the collapse of the total population. This  
214 collapse paradoxically determines its subsequent revival. (B) Revival is coupled to the  
215 endogenous emergence of variability in the composition of the groups (constituting the  
216 metapopulation) when the population is falling<sup>17,18</sup>, and the following occurrence of groups  
217 only constituted by cooperators (ecological Simpson's paradox). For the time window  
218 highlighted in (A), we display group composition (bottom; ratio of cooperators on each  
219 group is colored according to the gradient shown; white squares denote empty groups, of  
220 a total of  $N=30$ ), intergroup diversity (top; black curve, quantified as variance in group  
221 composition), and number of empty groups (top; pink curve). (C) To test experimentally  
222 these ideas, we engineered synthetic strains that contribute (green), or not (red), to the  
223 production of *quorum-sensing* (QS) molecules acting as an essential PG (fig. S2). A cell  
224 community that accumulates (top) or obtains (bottom) the PG in the environment is able  
225 to tolerate a bactericidal antibiotic stress (gentamicin, gm), although the latter can survive  
226 least because the initial PG is spent. Moreover, a community growing without PG would  
227 eventually collapse (middle). (D) Survival to gm of a population constituted only by  
228 cheaters increases when the essential QS molecules are added to the preincubation  
229 medium, before growing under the stress (8 $\mu$ g/ml gm,  $N=17$  replicas per QS dosage, solid  
230 color represent 95% confidence interval of a local polynomial regression). (E) Fraction of  
231 cooperators in a mixed population decays with time due to the invasion of cheaters, which  
232 do not pay the cost of making the PG (fig. S4). This is independent of the initial fraction  
233 (10% or 50% of cooperators). Boxes indicate standard deviation linked to the  
234 experimental estimation of ratios. See (Methods) for further details and protocols.

235

236 **Fig. 2.** Experimental test of the ecological Simpson's paradox. (A) Survival population to  
237 gentamicin (gm) exposure from an initial density of  $\sim 10^4$  cells/ml and different population  
238 composition. Cells grow for 15.5 hrs ( $T_1$ ) without stress to be then 1/10 reseeded in a



239 medium with 8 $\mu$ g/ml of gm, in which they grow 8.5 hrs ( $T_2$ ) (Methods). Each dot  
240 represents a single replica ( $N=45$ ), and box plots represent associated statistical  
241 parameters. Cooperators/cheaters labelled as producers (P)/nonproducers(nP) of the  
242 public good, respectively. (Right inset) Accumulation of *quorum-sensing* molecules (QS)  
243 at  $T_1$ ; population constituted by 20% or all Ps (Methods). (B) Survival population to three  
244 gm dosages. Initial density of  $\sim 10^4$  cells/ml, with a composition of 20% Ps. Dots and box  
245 plots as in (A),  $N=45$ . Population densities, and associated dosages of 9.5 $\mu$ g/ml and  
246 13 $\mu$ g/ml, are correspondingly termed as "pop 1" and "pop 2" conditions. The frequency of  
247 P remains approximately the same at the end of the protocol (fig. S6). (C) Cartoon of a  
248 second round of the experimental protocol. Initial conditions correspond to those of either  
249 "pop 1" or "pop2" in (B). Each population is first distributed in a multiwell plate  
250 representing a metapopulation, followed by a period of accumulation of QS ( $T_1$ ) and  
251 stress ( $T_2$ ), as before (low initial densities on each well are represented here by weak  
252 opacity). The population is then quantified by plating and considered as a whole (merged  
253 metapopulation). Note the enrichment of groups of nPs for the "pop 2" experimental  
254 condition, and also the appearance of some groups constituted by only Ps. (D) Groups of  
255 Ps tolerate better the stress than groups of nPs, and lead to the recovery of the  
256 cooperation. We quantified the characteristic tolerance by engineering replica populations  
257 of only Ps and only nPs with the "pop 1" and "pop 2" associated cell densities and gm  
258 dosages, and then measured recovery of each well (each dot represents the fate of a  
259 replica well,  $N=45$ ). A maximal value of  $\sim 10000$  cfu/well denotes very strong recovery.  
260 Mixed wells with low initial density normally exhibit the fate of nPs at these high dosages  
261 (fig. S8). Note that nPs show almost no recovery in the "pop 2" conditions (bottom, gm =  
262 13 $\mu$ g/ml). See also main text.

263

264 **Fig. 3.** Additional constraints influence the maintenance of public good-based  
265 communities under antibiotic stress. (A) Cheater strains in exponential or saturating phase  
266 were resuspended in medium with gentamicin (gm) (Methods). (Right) Cells in  
267 exponential phase experienced less antibiotic tolerance<sup>23</sup> (gm =12 $\mu$ g/ml, dots correspond  
268 to  $N=45$  replicas, box plots indicate associated statistical parameters). (Left)  
269 Concentration of *quorum-sensing* (QS) molecules decays as a function of time of growth<sup>24</sup>

270 (figure S9), starting from an initial low-density of cooperators, i.e., "pop 2" density  
271 condition in Fig. 2. Bars represent measurement errors associated to QS estimation  
272 (Methods). Starting from these "pop 2" initial densities, and after an accumulation time of  
273 15.5 hrs ( $T_1$ ), cells are in exponential phase, and the amount of QS is maximal. Recovery  
274 is thus strongly linked to the presence of the public good (PG). **(B-C)** Emergence of  
275 spontaneous mutants to gm. Initial populations of cooperators and cheaters are subjected  
276 to an accumulation and stress protocol under the "pop 1" and "pop 2" conditions (same as  
277 Fig. 2; black dots represent replicas,  $N=45$ ; box plots represent statistical parameters,  
278 color codes as Fig. 2). We repeated the experiment for each strain and dosage, so that one  
279 can quantify the typical resulting population, and also the mutant subpopulation (by  
280 plating with -gm- and without -no gm- antibiotic; the specific plating dosage corresponds  
281 to that of the matching growing conditions). Emergence of spontaneous mutants is  
282 reduced at higher dosage (C). Tolerance is most significantly associated in this regime to  
283 the presence of the PG.

284

285

286

287

288

289

290

291

292

293

## 294 **Methods**

### 295 ***Ecological public good model***

296 We used a model first described in <sup>21</sup> to simulate the dynamics of a population whose  
297 growth is based on an essential public good (PG). It is based on a one-shot PG game<sup>27</sup>  
298 in which agents can contribute (“cooperators”) or not (“cheaters”) to the PG in  
299 groups of size  $N$ . Contributing implies a cost  $c$  to the agents. Group contributions are  
300 then summed, multiplied by a reward factor  $r$  (that determines the efficiency of the  
301 investments and the attractiveness of the PG) and redistributed to all group  
302 members, *irrespective* of their contribution. The PG game is characterized by the  
303 parameters  $N$ ,  $r$  and  $c$  (group size, efficiency and cost of the PG, respectively, where  
304 we fixed  $c = 1$  without loss of generality).

305 Every simulation starts with an initial population constituted by a common pool of  $k$   
306 identical agents in the *cooperator* state, where  $k$  is the maximal population size  
307 (carrying capacity), to be updated in a *sequential* way as follows (see also Figure S1):

308 (i) The common pool is divided in randomly formed groups of size  $N$  (i.e.  $N$  is the  
309 total number of individuals and empty spaces in each group). The number of formed  
310 groups is then  $\lfloor k/N \rfloor$ .

311 (ii) In each one of the (non-empty) groups, a one-shot PG game is played. This means  
312 that cheaters receive the payoff  $P_{\text{cheater}} = icr/(i + j)$ , while cooperators receive the  
313 same payoff minus a cost, i.e.  $P_{\text{cooperator}} = P_{\text{cheater}} - c$ ; with  $i, j$  being the number of  
314 cooperators and cheaters in the group, respectively, and  $i + j \leq N$ . After the  
315 interaction the grouping of individuals is dissolved.

316 (iii) Each individual can replicate (duplicate) with a probability that is calculated by  
317 dividing its payoff by the maximal possible one (i.e. the payoff obtained by a cheater  
318 in a group of  $N-1$  producers). Each cooperator that replicates generates an offspring  
319 that is either a cheater (with probability  $\nu$ ) or an identical cooperator (with  
320 probability  $1-\nu$ ).

321 (iv) Individuals are removed with probability  $\delta$  (individual death rate).

322 In simpler words, the life cycle of the computational model is characterized by two  
323 distinct *stages*. In stage I (steps i–ii), the population is structured in evenly sized  
324 randomly formed groups in which the PG game is played. In stage II (steps iii–iv,  
325 after groups disappear), each individual replicates according to the group  
326 composition (and payoff) experienced in stage I. Replication can happen only when  
327 the current total population is less than the maximal population size,  $k$ , i.e. there  
328 exists empty space (empty spaces are calculated by considering  $k$  minus the current  
329 amount of individuals in the population). If more individuals could replicate than the  
330 available empty space, only a random subset of them ultimately replicates (of size  
331 the number of empty spaces available).

### 332 ***Media, growth conditions and chemicals***

333 Strains were grown in LB broth (10gl<sup>-1</sup> casein peptone, 5gl<sup>-1</sup> yeast extract, and 5gl<sup>-1</sup>  
334 NaCl) at 30°C with constant shaking. Overnight cultures were grown aerobically in

335 flasks (170rpm) at 30°C, and experiments were performed in 96-well plates  
336 (Thermo Scientific, Denmark), with 200µl of medium, 50µl of mineral oil (Sigma-  
337 Aldrich, MO, USA), and shaking at 10000rpm and 30°C. Where indicated, antibiotics  
338 were added to the liquid medium or plate at final concentrations: kanamycin (Km)  
339 50µg/ml, spectinomycin (Sp) 50µg/ml in the construction of strains and 25µg/ml in  
340 experiments, and/or gentamicin (gm) with concentration as noted in the  
341 experiments. The synthetic *quorum-sensing* molecule N-butyryl-L-homoserine  
342 lactone (C4-HSL) was purchased from Cayman Chemical (Mi, USA). Cell dilutions  
343 were done in PBS (pH 7.4, 80.6mM Na<sub>2</sub>HPO<sub>4</sub>, 19.4mM KH<sub>2</sub>PO<sub>4</sub>, 27mM KCl, 1.37M  
344 NaCl at 10X, USB Corporation, OH, USA).

### 345 **Measurement of population size**

346 Cultures were spread onto 1.5% (w/v) agar plates with five 3mm glass beads for  
347 30s, and are incubated at 30°C for 48h (or otherwise indicated). Then, to quantify the  
348 cell number of a population we counted colony forming units (CFU) under blue light  
349 illumination (LED transilluminator, Safe Imager™ 2.0, Invitrogen, Waltham MA USA).  
350 The OD<sub>600</sub> of cultures was measured in a VICTOR2x 2030 Multilabel Reader machine  
351 (Perkin Elmer, Waltham, MA, USA) with intermittent orbital shaking. For  
352 experiments with P and nP strains, Km and Sp were added to the media.

### 353 **General DNA techniques, plasmids and strain constructions**

354 The different *E. coli* strains were derivatives of JC1080 (BW25113  $\Delta$ *sdi::FRT*)<sup>22</sup>.  
355 Oligonucleotides used in this work are indicated in Table S1. Plasmid DNA was  
356 prepared using the QIAprep Spin Miniprep kit (Qiagen, Inc., Valencia, CA). When  
357 required DNA was purified using the NucleoSpin Extract II (Macherey-Nagel, Düren,  
358 Germany). Colony PCR was performed by transferring cells directly from fresh agar  
359 plates into PCR reaction tubes.

360 The pZS4int-rhIL-GmLAA plasmid was constructed by PCR amplifying the *aacC1*  
361 gene (Gm<sup>R</sup>), from pSEVA611 plasmid<sup>28</sup>, to which 33-bp, encoding the  
362 AANDENYALAA protease degradation tag was added to the 3'-end using primers  
363 Gm-kpnI-F and GmLAA-hindIII-R (Table S1). The ~0.5-kb PCR DNA was digested  
364 with KpnI and HindIII and used to replace the ~0.7-kb fragment containing the  
365 *catLVA* resistance marker from pZS4int-rhl-catLVA<sup>22</sup> generating the pZS4int-rhIL-  
366 GmLAA plasmid. Thus, the "Genomic insert" parental strain was constructed by  
367 integrating the cassette T<sub>0</sub>-Sp<sup>R</sup>-*rhlR*←P<sub>lacIq</sub>-P<sub>rhl</sub>→Gm<sup>R</sup><sub>LAA</sub>-T<sub>1</sub> into the λ attachment site  
368 (*attB*) of *E. coli* JC1080 with the helper plasmid pLDR8, that bears the lambda  
369 integrase, as described<sup>29</sup>. The pZS4int-rhIL-GFP plasmid was assembled by  
370 extracting the *gfp* gene from pSEVA241-P<sub>rhl</sub>→*gfp* vector (lab collection) upon  
371 digestion with KpnI and HindIII. Then, the 0.7-kb DNA fragment was cloned into the  
372 KpnI and HindIII sites of pZS4int-rhIL-GmLAA replacing the Gm<sup>R</sup><sub>LAA</sub> cassette for a  
373 GFP fluorescent reporter.

374 Then, the quorum sensing reporter "biosensor" strain was constructed by  
375 introducing into the λ attachment site (*attB*) of *E. coli* JC1080 the cassette T<sub>0</sub>-Sp<sup>R</sup>-  
376 *rhlR*←P<sub>lacIq</sub>-P<sub>rhl</sub>→*gfp*-T<sub>1</sub> as described above. The plasmid pZS\*2R-GFP-rhII (ori-  
377 SC101\*, P<sub>R</sub>→*gfp-rhII*, Km<sup>R</sup>) was obtained from <sup>22</sup>. The pZS\*2R-mCherry (ori-SC101\*,  
378 P<sub>R</sub>→*gfp-rhII*, Km<sup>R</sup>) plasmid was constructed by amplifying *mcherry* from pSEVA237R

379 (4)(9) using primers mCherry-kpnI-F and mCherry-xbaI-R (Table S1). The PCR-  
380 amplified fragment was flanked with KpnI and XbaI restriction sites and cloned into  
381 the corresponding sites of the ~3.5-kb pZS\*2R-GFP-rhlI plasmid backbone, thereby  
382 swapping the *gfp-rhlI* cassette for the *mcherry* gene.

### 383 ***GFP expression assay to estimate QS signal concentration***

384 To estimate the concentration of the quorum sensing signal produced (C4-HSL), in  
385 different experimental conditions we used the reporter “biosensor” bacteria. We  
386 grew the “biosensor” strain overnight, adjusted the OD<sub>600</sub> to 0.1 and grew aerobically  
387 for 2.5h at 30°C. Then, the culture was aliquoted and purified supernatant from the  
388 experimental sample was added. We used known concentrations (0, 0.1μM, 1μM,  
389 10μM, and 100μM) of the commercial N-butyryl-L-homoserine lactone (C4-HSL) to  
390 obtain a calibration curve. We grew these preparations aerobically for 3h, laid out  
391 200 μl of cultures in quadruplicates in a 96-well black/clear bottom microtiter plate  
392 (Sigma-Aldrich, MO, USA) and measured OD<sub>600</sub> and GFP fluorescence (ex: 488nm;  
393 em: 520nm; cutoff: 495nm) in a SpectraMax M2<sup>e</sup> microplate reader (Molecular  
394 Devices, CA, USA). Supernatants were obtained from 200μl of overnight liquid  
395 cultures prepared following the “Accumulation of PG and stress” protocol,  
396 centrifuged twice at room temperature to remove cells and used directly to induce  
397 growing cells of the reporter strain. Comparing observed supernatant fluorescence  
398 to the calibration curve approximated QS molecule quantities.

### 399 ***Engineering of initial conditions***

400 Initial populations for the “accumulation of PG and stress” protocol and others were  
401 prepared by mixing cooperators and cheaters at a defined population density (10<sup>4</sup>  
402 cells/well for high initial density experiments and 1-10 cell/well for low initial  
403 density experiments) and cooperator frequency. Overnight cultures of producers  
404 and nonproducers were washed twice with PBS by centrifugation for 15min at  
405 3800rpm and room temperature. Then, OD<sub>600</sub> was adjusted to 0.15. We assembled  
406 populations at the desired P frequency in a fixed final volume (2.5ml), which was  
407 then serially diluted to the required cell density. This dilution was done in large  
408 volumes of medium (20ml) and applying low dilution factor (¼) each step to  
409 minimize the introduction of error in strain frequencies. Initial dilution steps were  
410 performed in PBS and the final 3 steps were performed in LB with Km, Sp. The  
411 robustness of this procedure is shown in Fig. S5.

### 412 ***Invasion of nonproducers***

413 We prepared washed cultures of producers and nonproducers as described above.  
414 After adjusting OD<sub>600</sub>, to 0.15 we mixed both strains at the indicated frequency. Then,  
415 we inoculated three replica 50ml Erlenmeyer flasks with 5ml of LB, Km, Sp. After  
416 24h, we reseeded a new flask with a 1/100 dilution and fresh medium. In order to  
417 estimate producer frequency in grown cultures, cells were 1/10 serially diluted in  
418 PBS using a total of 10ml of medium, plated onto LB agar plates, and colonies  
419 counted after 24h at 30°C. We followed this process for 4 consecutive days.

### 420 ***“Accumulation of PG and stress”***

421 Populations with a given initial cell density and cooperator frequency were  
422 prepared, distributed into a 96-multiwell plate and incubated for 15.5h ( $T_1$ ). Then,  
423 1/10 of each well was transferred into a new 96-multiwell plate with LB, Km, Sp and  
424 the specified gm concentration. This plate is again incubated for 8.5h ( $T_2$ ). At the end  
425 of  $T_2$  we plated whole well content on LB agar plates and counted CFU after 48hrs at  
426 30°C.

#### 427 ***Antibiotic sensitivity***

428 Overnight cultures were reseeded and grown for 4h at 30°C to reach exponential  
429 phase. Aliquots of this culture containing  $\sim 10^6$  cells were resuspended into a 96-  
430 multiwell plate with LB and a given dose of gm, incubated for 2h or 4h, plated and  
431 counted. For experiments with the nP strain, Km and Sp were added to the LB  
432 medium. For experiments with cells in stationary phase, overnight cultures were  
433 used directly in the initial inoculation. We used additional wells without antibiotic in  
434 parallel to obtain a reference population size. We express the sensitivity to the  
435 antibiotic as “fraction surviving” (population size after exposure to antibiotic /  
436 reference population size without antibiotic).

#### 437 ***Effect of synthetic quorum-sensing on gentamicin tolerance***

438 Overnight cultures of nonproducers were resuspended into LB with Km, Sp and the  
439 indicated concentrations of synthetic *quorum-sensing* molecule (C4-HSL). Then, we  
440 proceeded with the antibiotic sensitivity assay as described above.

#### 441 ***Mutation rate***

442 We generated replica populations of the nP strain and initial density of  $\sim 1$  cell/well.  
443 We distributed these cultures in 96-multiwell plates and allowed them to grow for  
444 15.5h ( $T_1$ ). We plated the whole well content on LB agar plates with the specified gm  
445 dosage and counted viable cells. From the distribution of  $gm^R$  CFU observed in a set  
446 of replica populations the mutation rate was estimated with a maximum likelihood  
447 method as described in<sup>30</sup>, using the online application “FALCOR: Fluctuation Analysis  
448 Calculator”  
449 (<http://www.keshavsingh.org/protocols/FALCOR.html> )

450

451

452

453

454

455

456

457

458

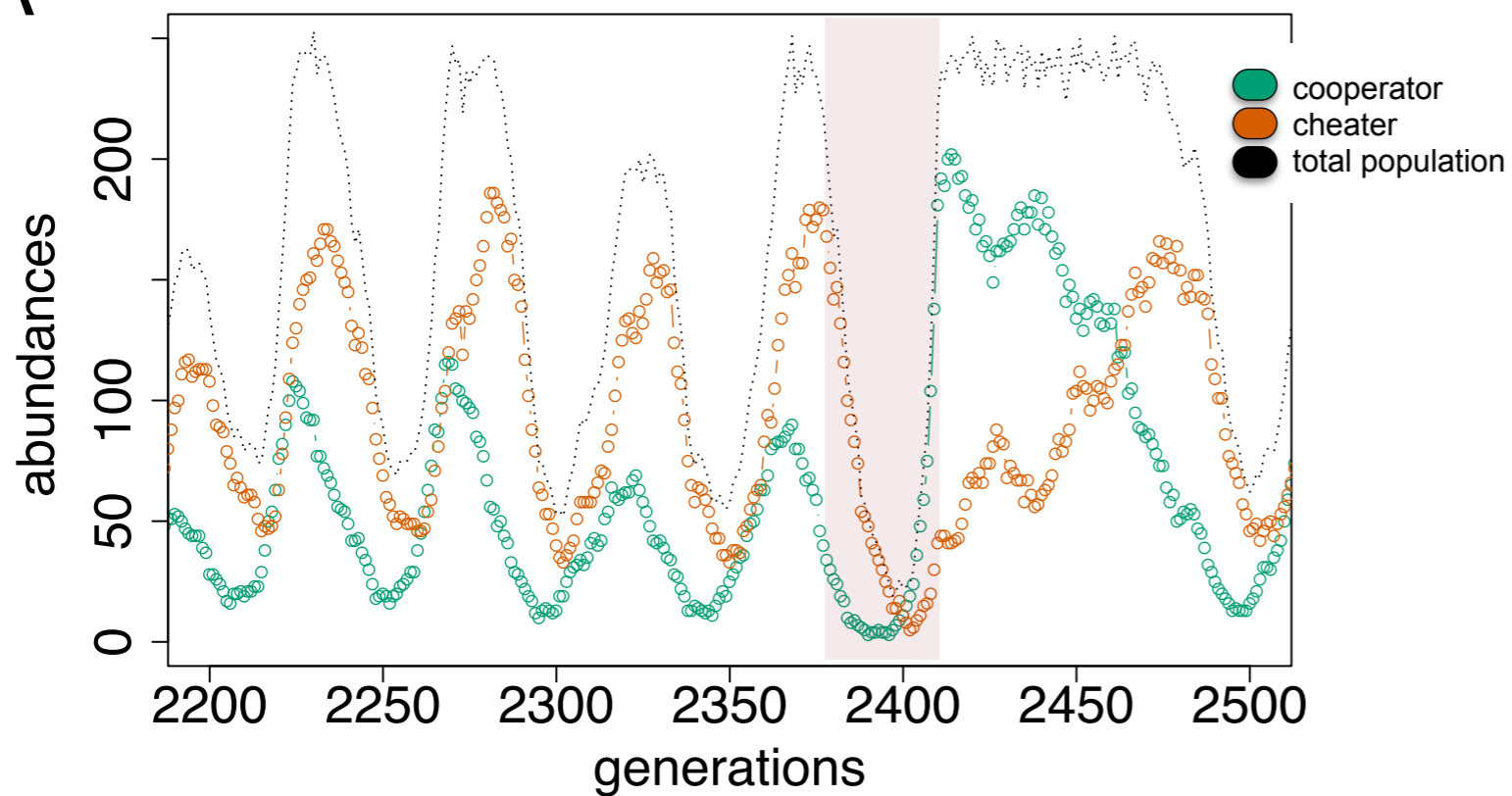
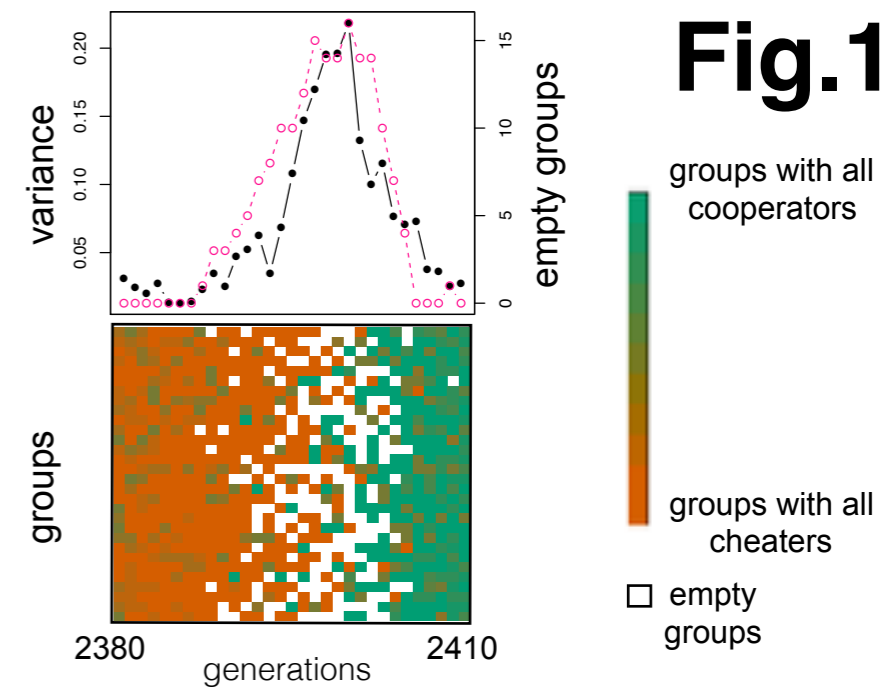
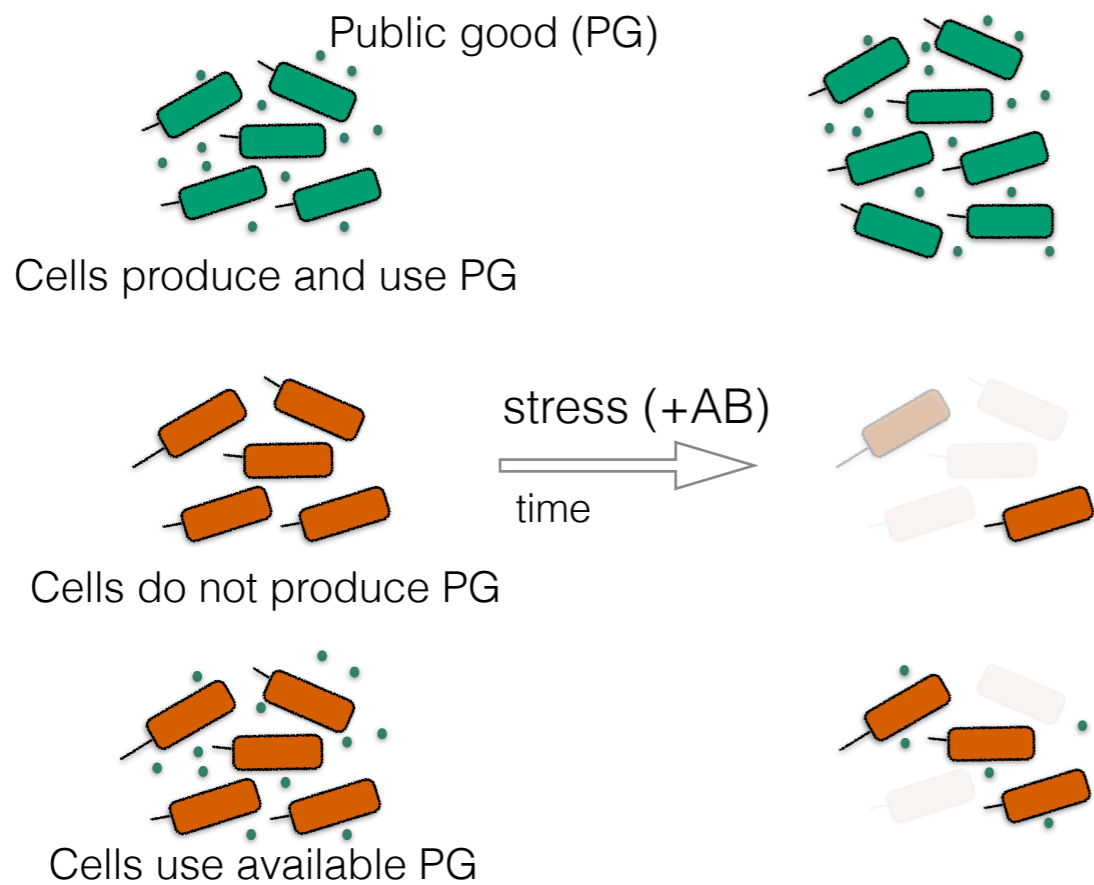
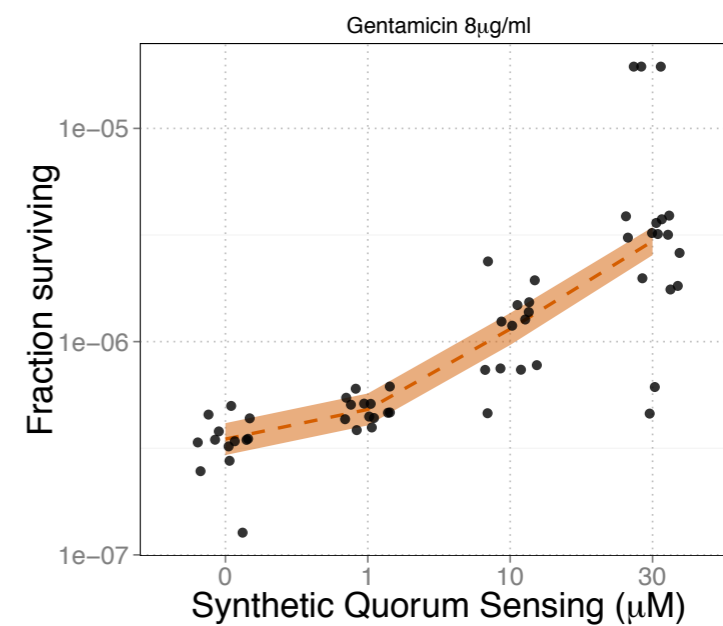
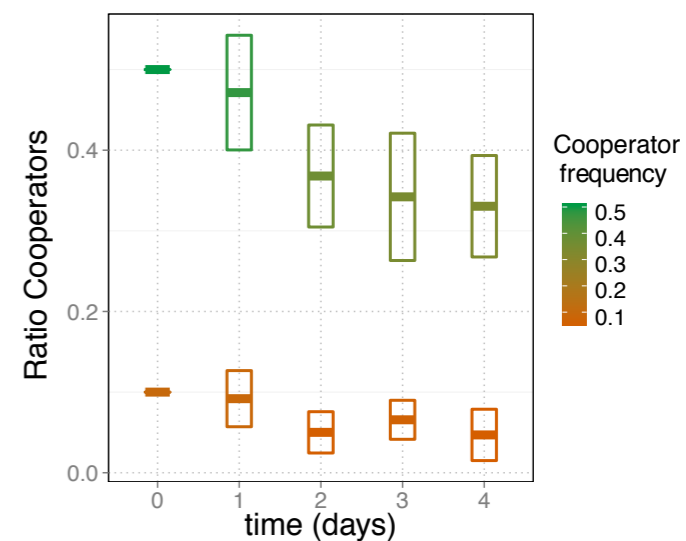
## 459 **References**

- 460 1. Waters, C. M, & Bassler, B. L. Quorum sensing: cell-to-cell communication in  
461 bacteria. *Annu Rev Cell Dev Biol* **21**, 319 (2005).
- 462 2. Nadell, C. D., Xavier, J. B. & Foster, K. R. The sociobiology of biofilms. *FEBS*  
463 *Microbiol Rev* **33**, 206 (2009).
- 464 3. Cordero, O. X. *et al.* Public good dynamics drive evolution of iron acquisition  
465 strategies in natural bacterioplankton populations. *Proc Natl Acad Sci USA* **109**,  
466 20059 (2012).
- 467 4. Gore, J. *et al.* Snowdrift game dynamics and facultative cheating in yeast. *Nature*  
468 **459**, 253 (2009).
- 469 5. Sandoz, K. M., Mitzimberg, S. M. & Schuster, M. Social cheating in  
470 *Pseudomonas aeruginosa* quorum sensing. *Proc Natl Acad Sci USA*, **104** (2007).
- 471 6. Hammerschmidt, K., Rose, C. J., Kerr, B. & Rainey, P. B. Life cycles, fitness  
472 decoupling and the evolution of multicellularity. *Nature* **515**, 75 (2014).
- 473 7. Travisano, M. & Velicer, G. J. Strategies of microbial cheater control. *Trends*  
474 *Microbiol* **12**, 72 (2004).
- 475 8. Frank, S. A. Microbial Evolution: Regulatory Design Prevents Cancer-like  
476 Overgrowths. *Curr Biol* **9**, R343 (2013).
- 477 9. Hardin, G. The Tragedy of the Commons. *Science* **162**, 1243 (1968).
- 478 10. Rakoff-Nahoum, S., Coyne, M. J. & Comstock, L. E. An ecological network of  
479 polysaccharide utilization among human intestinal symbionts. *Curr Biol* **24**, 40  
480 (2014).
- 481 11. Nair A, Juwarkar A. A. & Singh S. K. Production and characterization of  
482 siderophores and its application in arsenic removal from contaminated soil. *Water*  
483 *Air Soil Pollut.* **180**, 199–212 (2007).
- 484 12. Hamilton, W. D. *Narrow Roads of Gene Land, Vol 1* (Oxford Univ Press, Oxford,  
485 UK, 2006).

- 486 13. Nowak, M. A. Five Rules for the Evolution of Cooperation. *Science* **314**, 1560  
487 (2006).
- 488 14. Drescher, K. *et al.* Solutions to the public goods dilemma in bacterial biofilms.  
489 *Curr Biol* **24**, 50 (2014).
- 490 15. Julou, T. *et al.* Cell-cell contacts confine public goods diffusion inside  
491 *Pseudomonas aeruginosa* clonal microcolonies. *Proc Natl Acad Sci USA* **110**,  
492 12577 (2013).
- 493 16. Nowak, M. A. *Evolutionary Dynamics: Exploring the Equations of Life*. (Harvard  
494 Univ Press, Cambridge, MA, USA, 2006).
- 495 17. Hauert, C., Holmes, M. & Doebeli, M. Evolutionary games and population  
496 dynamics: maintenance of cooperation in public goods games. *Proc R Soc B* **273**,  
497 3131 (2006).
- 498 18. Cavaliere, M. & Poyatos, J. F. Plasticity facilitates sustainable growth in the  
499 commons. *J R Soc Interface* **10**, 20121006 (2013).
- 500 19. Pai, A., Tanouchi, Y. & You, L. Optimality and robustness in quorum-sensing  
501 (QS)-mediated regulation of a costly public good enzyme. *Proc Natl Acad Sci*  
502 *USA* **109**, 19810 (2012).
- 503 20. Sánchez, A. & Gore, J. Feedback between Population and Evolutionary Dynamics  
504 Determines the Fate of Social Microbial Populations. *PLoS Biol* **11**, e1001547  
505 (2013).
- 506 21. Kerr, B. *et al.* Local migration promotes competitive restraint in a host-pathogen  
507 “tragedy of the commons”. *Nature* **442**, 75 (2006).
- 508 22. Chuang, J. S. *et al.* Simpson's Paradox in a Synthetic Microbial System. *Science*  
509 **323**, 272 (2009).
- 510 23. Fridman, O. *et al.* Optimization of lag time underlies antibiotic tolerance in  
511 evolved bacterial populations. *Nature* **513**, 418 (2014).
- 512 24. Byers, J. T. *et al.* Nonenzymatic turnover of an *Erwinia carotovora* quorum-  
513 sensing signaling molecule. *J Bacteriol* **184**, 1163 (2002).

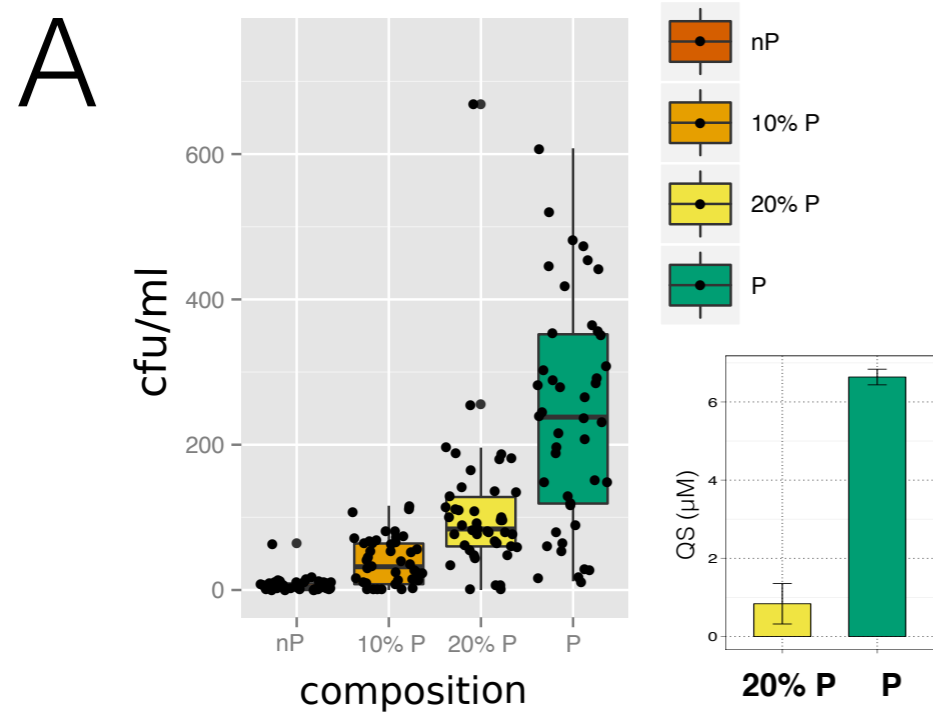


- 514 25. MacLean, R. C. & Buckling, A. The Distribution of Fitness Effects of beneficial  
515 Mutations in *Pseudomonas aeruginosa*. *PLoS Gen* **5**, e1000406 (2009).
- 516 26. Koch, H. *et al.* Why rapid, adaptive evolution matters for community dynamics.  
517 *Front Ecol Evol* **2**, 1 (2014).
- 518 27. Archetti M. & Scheuring I., Game theory of public goods in one-shot social  
519 dilemmas without assortment. *J Theor Biol* **299**, 9 (2012).
- 520 28. Silva-Rocha R. *et al.*, The Standard European Vector Architecture (SEVA): a  
521 coherent platform for the analysis and deployment of complex prokaryotic  
522 phenotypes. *Nucleic Acids Res* **41**, D666 (2012).
- 523 29. Lutz R. & Bujard H., Independent and tight regulation of transcriptional units in  
524 *Escherichia coli* via the LacR/O, the TetR/O and AraC/I1-I2 regulatory elements.  
525 *Nucleic Acids Res* **25**, 1203 (1997).
- 526 30. Foster P.L., Methods for determining spontaneous mutation rates. *Methods*  
527 *Enzymol*, **409**, 195 (2006).

**A****Population Dynamics****B****C****D****E**

**Fig.2**

Effect of population composition



Effect of stress dosage

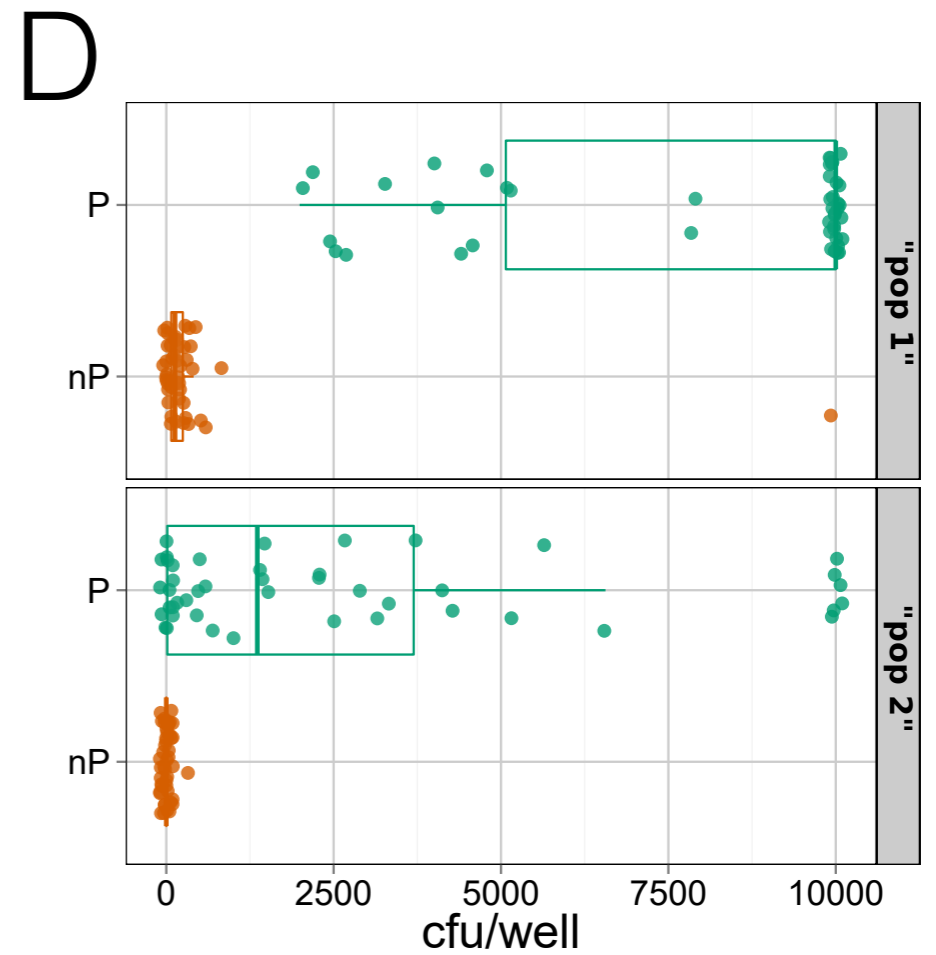
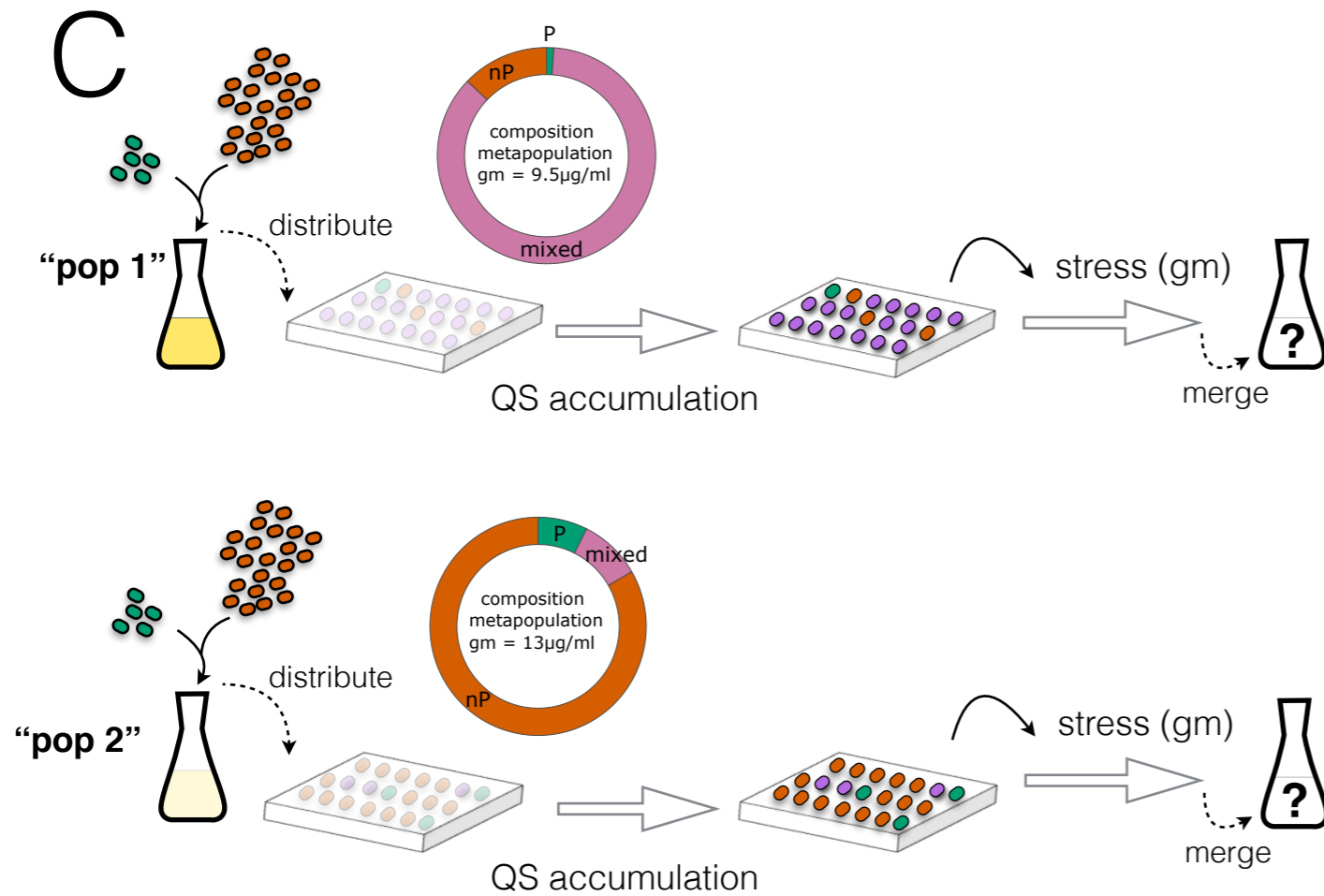
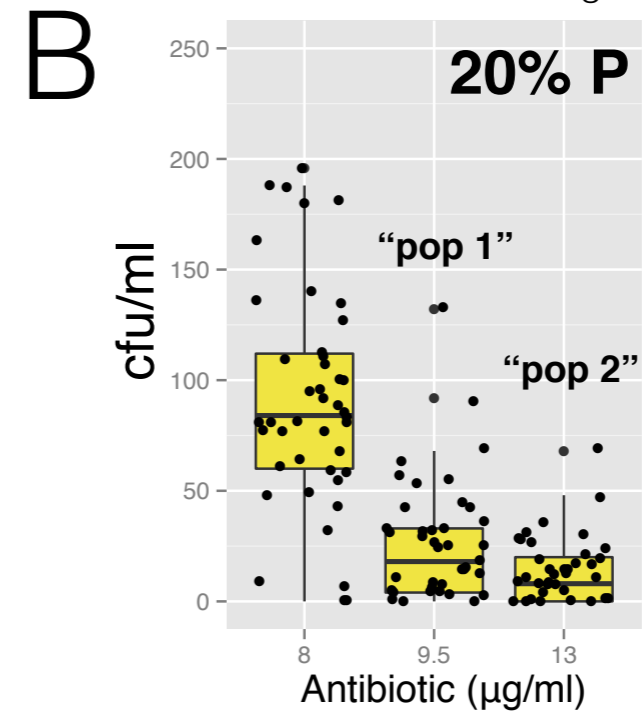
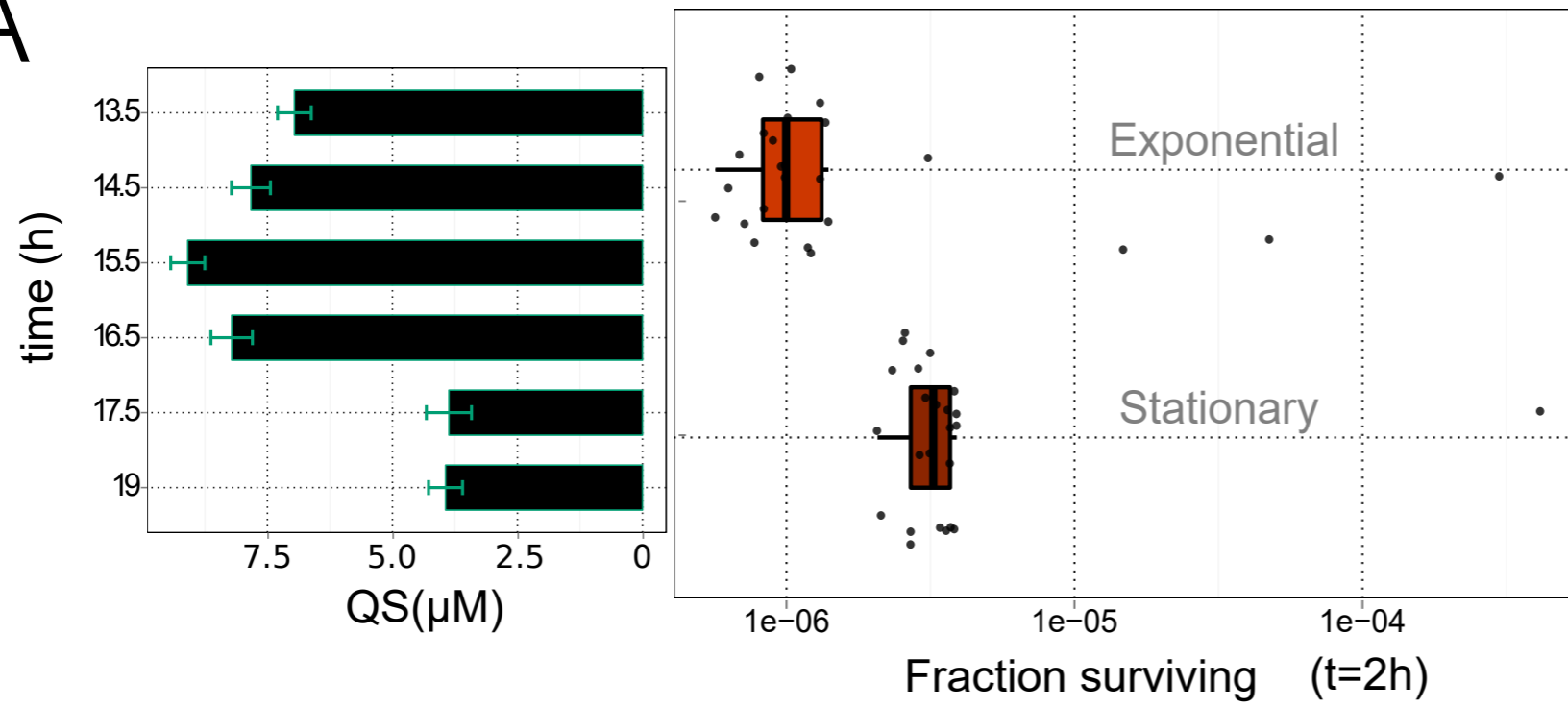
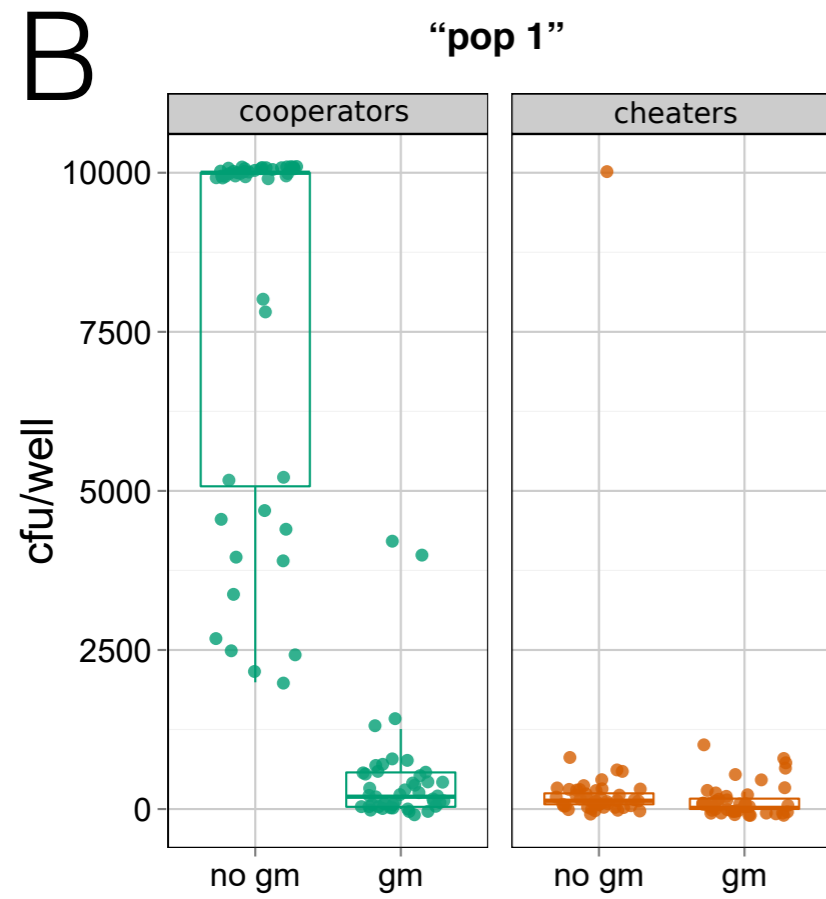


**Fig.3**

**A**



**B**



**C**

